

# Inelastic Electron Tunneling Spectroscopy and Vibrational Coupling

Liuming Yan\*

Department of Chemistry, College of Sciences, Shanghai University, 99 Shangda Road, Shanghai 200444, China

Received: July 23, 2006; In Final Form: September 6, 2006

We discuss the relationship between the inelastic electron tunneling spectroscopy (IETS) and vibronic coupling constant within the Green's function formalism at a level of perturbation theory approximation. We also compare our results with experimental measurements. Our results can provide insights into the mechanism of active vibronic modes for IETS.

## 1. Introduction

Inelastic electron tunneling spectroscopy (IETS) is an important tool for identifying molecular species in tunneling junctions.<sup>1,2</sup> It is also a technique with ultrahigh sensitivity, even single molecular IETS can be observed with a scanning tunneling microscope (STM).<sup>3,4</sup> Recently, IETS attracted considerable research interest in the molecular electronics community.<sup>5–7</sup> Indeed, IETS is the only direct way to ascertain that a molecule participates in the conduction process,<sup>8</sup> because its spectroscopic information can be verified using independent spectroscopic techniques such as IR or Raman spectroscopy.

Several theoretical approaches to the explanation and prediction of IETS exist in literature.<sup>9</sup> The most used approach is based on perturbative theory.<sup>1,10,11</sup> Perturbative approach has been used to interpret IETS of model systems,<sup>10</sup> small molecules on surfaces,<sup>12</sup> and molecular wires.<sup>13</sup> The perturbative theory can provide a rough estimation and a qualitative explanation to some characteristics of IETS.<sup>8</sup> However, more sophisticated approaches are needed to accurately calculate IETS of molecules that are important to molecular electronics. Among these approaches, the nonequilibrium Green's function formalism<sup>9,14–19</sup> is by far the most used approach because it can provide a systematic framework for both elastic electron tunneling and inelastic electron tunneling.

In this paper, we develop an approach relating the IETS and the electronic–vibronic coupling by combining the perturbative theory and Green's function theory. The Green's function is evaluated by following Dyson's equation with the electronic–vibronic coupling, responsible for the IETS, as the perturbative to the junction, and the current as well as the IETS is calculated by use of the Landauer formalism. The vibronic analyses are carried out using density functional theory, and the electronic–vibronic coupling constant is evaluated using normal mode projection to the curvilinear coordinates. One advantage of this formalism is that the full Green's function as well as the electric current is evaluated as the summation of an elastic tunneling term and several inelastic tunneling terms, therefore, contribution from elastic tunneling and inelastic tunneling are separated. The other advantage is that the IETS peak height is the product of a slow change factor corresponding to the background independence of electronic–vibronic coupling and a factor directly correlated to the electronic–vibronic coupling.

This paper is arranged as follows: we describe our formalism in section 2, we give our calculation results in section 3, and summarize in the last section, section 4.

## 2. Formalism

**2.1 Physical Model.** To investigate the inelastic electron tunneling spectroscopy through a molecular junction that is composed of two metallic leads serving as reservoirs of electrons and a molecule serving as bridge, we divide the Hamiltonian operator of the molecule  $\hat{H}$  into two parts

$$\hat{H} = \hat{H}_{\text{el}} + \hat{H}_{\text{inel}} \quad (1)$$

where  $\hat{H}_{\text{el}}$  is responsible for elastic electron tunneling and  $\hat{H}_{\text{inel}}$  is responsible for inelastic electron tunneling. Under the Born–Oppenheimer approximation, electronic and vibronic contribution to the Hamiltonian operator  $\hat{H}_{\text{el}}$  can be separated

$$\hat{H}_{\text{el}} = \sum_{n=1}^N \epsilon_n \hat{c}_n^+ \hat{c}_n + \sum_{m=1}^M hc \nu_m \hat{a}_m^+ \hat{a}_m \quad (2)$$

Here,  $\epsilon_n$  is the electronic level in the molecule;  $\hat{c}_n$  and its adjoints are the annihilation and creation operators of electrons in electronic level  $n$ ;  $N$  is the total number electrons,  $c$  is speed of light,  $\nu_m$  is wavenumber of molecular vibrational mode  $m$ ,  $\hat{a}_m$  and its adjoints are annihilation and creation operators of phonons,  $M$  is the number of vibrational modes in the molecule, and  $h$  is the Plank constant. The electronic–vibronic coupling  $\hat{H}_{\text{inel}}$  is<sup>17,18</sup>

$$\hat{H}_{\text{inel}} = \sum_{m,n} \lambda_{m,n} (\hat{a}_m^+ + \hat{a}_m) \hat{c}_n^+ \hat{c}_n \quad (3)$$

where  $\lambda_{m,n}$  is the electronic–vibronic coupling constant between a vibronic mode  $m$  and an electronic state  $n$ .

By omitting the electronic–vibronic coupling, we get the retarded Green's function  $\hat{G}_{\text{el}}^{\text{R}}(E)$  responsible for elastic electron tunneling

$$\hat{G}_{\text{el}}^{\text{R}}(E) = (E\hat{I} - \hat{H}_{\text{el}} - \hat{\Sigma}_{\text{L}} - \hat{\Sigma}_{\text{R}})^{-1} \quad (4)$$

Here,  $E$  is the energy of the tunneling electron,  $\hat{I}$  is the unit operator, and  $\hat{\Sigma}_{\text{L}}$  and  $\hat{\Sigma}_{\text{R}}$  are the self-energies of the left and right leads. Treating the electronic–vibronic coupling as a small

\* E-mail: liuming.yan@shu.edu.cn.

perturbation, the full retarded Green's function

$$\hat{G}^R(E) = (E\hat{I} - \hat{H}_{\text{el}} - \hat{\Sigma}_{\text{L}} - \hat{\Sigma}_{\text{R}} - \hat{H}_{\text{inel}})^{-1} \quad (5)$$

could be evaluated by the following Dyson's equation:

$$\hat{G}^R(E) = \hat{G}_{\text{el}}^R(E) + \hat{G}_{\text{el}}^R(E)\hat{H}_{\text{inel}}\hat{G}^R(E) \quad (6)$$

Keeping only the first-order approximation, we get

$$\hat{G}^R(E) = \hat{G}_{\text{el}}^R(E) + \hat{G}_{\text{el}}^R(E)\hat{H}_{\text{inel}}\hat{G}_{\text{el}}^R(E) \quad (7)$$

**2.2 IETS Formalism.** Because the inelastic interaction is very small compared to the elastic interactions, the Landauer–Büttiker equation<sup>20–22</sup> still applies, and the current is evaluated

$$I = \frac{2e}{h} \int_{-\infty}^{\infty} T(E, V) (f_{\text{L}}(E, V_{\text{L}}) - f_{\text{R}}(E, V_{\text{R}})) dE \quad (8)$$

Here  $V_{\text{L}}$  and  $V_{\text{R}}$  are electric bias applied to the left and right leads,  $V = V_{\text{R}} - V_{\text{L}}$ ,  $f_{\text{L,R}}(E, V_{\text{L,R}})$  are the Fermi distribution functions of the left and right leads at bias  $V_{\text{L,R}}$ ,  $e$  is the elementary charge unit, and  $T(E, V)$  is the electron transmission function calculated from the Green's function<sup>23</sup>

$$T(E, V) = \text{tr}(\hat{\Gamma}_{\text{L}}\hat{G}^R(E)\hat{\Gamma}_{\text{R}}\hat{G}^A(E)) \quad (9)$$

where  $\hat{G}^A(E)$  is the advanced Green's function, and  $\hat{\Gamma}_{\text{L}}$  and  $\hat{\Gamma}_{\text{R}}$  are the imaginary part of the self-energies of the left and right leads

$$i\hat{\Gamma}_{\text{L,R}} = \hat{\Sigma}_{\text{L,R}}^+ - \hat{\Sigma}_{\text{L,R}} \quad (9)$$

Here  $\hat{\Sigma}_{\text{L,R}}^+$  is the adjoint of  $\hat{\Sigma}_{\text{L,R}}$ . At low temperature, the Fermi distribution function is almost a step function, and the current could be approximated by<sup>24</sup>

$$I = \frac{2e}{h} \int_{E_{\text{F}}+V_{\text{L}}}^{E_{\text{F}}+V_{\text{R}}} T(E, V) dE \quad (10)$$

Apply the full Green's function to this equation and neglect the small last term, we get

$$I = \frac{2e}{h} \int_{E_{\text{F}}+V_{\text{L}}}^{E_{\text{F}}+V_{\text{R}}} \text{tr}(\hat{\Gamma}_{\text{L}}\hat{G}_{\text{el}}^R\hat{\Gamma}_{\text{R}}\hat{G}_{\text{el}}^A + \hat{\Gamma}_{\text{L}}\hat{G}_{\text{el}}^R\hat{\Gamma}_{\text{R}}\hat{G}_{\text{el}}^A\hat{H}_{\text{inel}}\hat{G}_{\text{el}}^A + \hat{\Gamma}_{\text{L}}\hat{G}_{\text{el}}^R\hat{H}_{\text{inel}}\hat{G}_{\text{el}}^R\hat{\Gamma}_{\text{R}}\hat{G}_{\text{el}}^A) dE \quad (11)$$

where  $\hat{\Gamma}_{\text{L,R}}$  and  $\hat{G}_{\text{el}}^{\text{R,A}}$  depend on energy,  $\hat{H}_{\text{inel}}$  depends on both the energy and the frequency of the vibration, and the differential conductance  $g$  is

$$g = \frac{2e^2}{h} \text{tr}(\hat{\Gamma}_{\text{L}}\hat{G}_{\text{el}}^R\hat{\Gamma}_{\text{R}}\hat{G}_{\text{el}}^A + \hat{\Gamma}_{\text{L}}\hat{G}_{\text{el}}^R\hat{\Gamma}_{\text{R}}\hat{G}_{\text{el}}^A\hat{H}_{\text{inel}}\hat{G}_{\text{el}}^A + \hat{\Gamma}_{\text{L}}\hat{G}_{\text{el}}^R\hat{H}_{\text{inel}}\hat{G}_{\text{el}}^R\hat{\Gamma}_{\text{R}}\hat{G}_{\text{el}}^A) \quad (12)$$

Here, the total conductance is evaluated by the elastic electron tunneling (first term)

$$g_{\text{el}} = \frac{2e^2}{h} \text{tr}(\hat{\Gamma}_{\text{L}}\hat{G}_{\text{el}}^R\hat{\Gamma}_{\text{R}}\hat{G}_{\text{el}}^A) \quad (12A)$$

and inelastic electron tunneling (the other two terms)

$$g_{\text{inel}} = \frac{2e^2}{h} \text{tr}(\hat{\Gamma}_{\text{L}}\hat{G}_{\text{el}}^R\hat{\Gamma}_{\text{R}}\hat{G}_{\text{el}}^A\hat{H}_{\text{inel}}\hat{G}_{\text{el}}^A + \hat{\Gamma}_{\text{L}}\hat{G}_{\text{el}}^R\hat{H}_{\text{inel}}\hat{G}_{\text{el}}^R\hat{\Gamma}_{\text{R}}\hat{G}_{\text{el}}^A) \quad (12B)$$

Inelastic electron tunneling represents a small net change to the conductance of the molecular device, which is mainly contributed by the elastic electron tunneling. This change in conductance is the IETS signal  $\eta_{\text{inel}}^2$

$$\eta_{\text{inel}} = \frac{1}{g} \left( \frac{dg}{dV} \right)_{\text{inel}} \quad (13)$$

Because the inelastic tunneling is very weak compared to elastic tunneling ( $g = g_{\text{el}} + g_{\text{inel}} \approx g_{\text{el}}$ ) and the differential conductance of elastic tunneling is slow changing with applied voltage compared to that of the inelastic tunneling vicinity to a vibrational peak of the IETS ( $dg_{\text{el}}/dV \approx 0$ ), thus, eq 13 can be evaluated by

$$\eta_{\text{inel}} \approx \frac{1}{g_{\text{el}}} \left( \frac{dg_{\text{inel}}}{dV} \right) \quad (13A)$$

When we consider the case that only one channel contributed to conduction, all operators in eq 12 could be written as scalars and the IETS is evaluated as

$$\eta_{\text{inel}} \approx \frac{d(G_{\text{el}}^A + G_{\text{el}}^R)H_{\text{inel}}}{dV} \quad (14)$$

or

$$\eta_{\text{inel}} = (G_{\text{el}}^A + G_{\text{el}}^R) \sum_{m=1}^M e\lambda_m^2 \delta\left(\frac{eV}{hc} - \nu_m\right) \quad (15)$$

where  $(G_{\text{el}}^A + G_{\text{el}}^R)$  is a slow-changing function representing the background of the IETS,  $\lambda_m$  is the electronic–vibronic coupling constant between vibrational mode  $m$  and the conduction channel, and  $\delta(eV/hc - \nu_m)$  is Dirac's delta function.

In the next section, we will discuss the calculation of the vibrational frequencies and the electronic–vibronic coupling constant using density functional theory.

### 3. Numerical Calculations

**3.1 Vibrational Modes.** The Gaussian 2003 program<sup>25</sup> is used for the calculation of vibrational modes at theoretical level of Kohn–Sham (KS) formalism,<sup>26,27</sup> with the Becke-3 hybrid exchange functional,<sup>28</sup> the generalized-gradient approximation Perdew–Wang correlation functional,<sup>29,30</sup> and the LANL2DZ basis sets, with effective core potentials.<sup>31–33</sup> The molecular geometries are optimized to local minima confirmed by analytic secondary derivatives calculation.<sup>34</sup> The vibrational frequencies are calculated at the same level of theory.

The ab initio harmonic frequencies are generally overestimated because of the incomplete treatment of electron correlation, neglecting of mechanical anharmonicity, and basis set truncation effects.<sup>35–37</sup> The ab initio harmonic frequencies are improved by scaling<sup>38</sup>

$$\nu_m = f_{\text{scale}} \nu_{m,\text{harmonic}} \quad (16)$$

The scaling could use several parameters,<sup>39,40</sup> dual parameters,<sup>41,42</sup> or a uniform parameter.<sup>38,42,43</sup> In this paper, a scaling factor of 0.95 is used, which gives a comparable wavenumber with experimental results.<sup>44</sup>

**3.2 Electronic–Vibronic Coupling Constant.** The electronic–vibronic coupling constant  $\lambda_m$  is calculated using<sup>45</sup>

$$\lambda_m = |q_m| \nu_m \quad (17)$$

## SCHEME 1

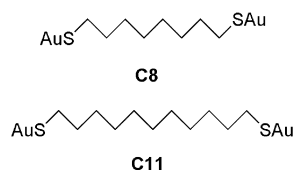


**TABLE 1: Major Normal Mode Displacements of the Positively Charged States of C8 and C11 Relative to the Neutral Molecule**

C8		C11	
$\nu$ (cm <sup>-1</sup> )	$q$	$\nu$ (cm <sup>-1</sup> )	$q$
28	0.004	10	0.071
39	-0.342	15	-0.004
78	0.406	35	0.003
180	-0.289	44	0.394
292	-0.280	45	0.001
372	-0.273	68	-0.001
439	-0.017	88	-0.216
675	-0.138	94	-0.002
959	-0.033	166	0.001
1023	-0.011	174	-0.393
1053	0.017	259	0.278
1055	-0.022	266	0.002
1202	-0.245	350	0.233
1264	0.166	386	-0.023
1319	0.059	477	0.156
1339	-0.013	670	-0.120
1429	0.081	672	-0.004
1438	-0.010	960	0.019
1442	0.010	982	-0.024
1454	-0.021	1030	0.011
2882	-0.010	1052	-0.006
2887	-0.009	1068	0.037
2906	0.012	1194	-0.204
2954	0.033	1236	-0.192
		1289	0.111
		1323	-0.049
		1339	-0.008
		1429	0.029
		1429	0.073
		1437	-0.008
		1441	0.005
		1443	0.019
		1453	-0.018
		1461	-0.007
		2879	0.004
		2883	0.009
		2886	-0.008
		2894	0.003
		2907	-0.010
		2954	-0.024
		2954	-0.022

Here  $q_m$  is the normal mode displacement of the charged conduction state from the neutral equilibrium state. The normal mode displacement is evaluated by the projection of the normal mode to the curvilinear coordinates using the DUSHIN program.<sup>46</sup>

**3.3 Examples.** To compare the theoretical IETS based on the electronic–vibronic coupling constant with the experimental IETS, we studied gold octanedithiolate (**C8**) and gold undecanedithiolate (**C11**; Scheme 1); the IETS of these two molecules have been studied experimentally.

Although several molecular orbitals may contribute to conduction, both junctions are supposed to be hole-conduction.<sup>47</sup> This hypothesis is based on the facts that the experimental barriers for alkane junctions are about 1.42 eV for a tunneling model,<sup>48</sup> and the intrinsic barriers corresponding to the energies of the molecular orbitals in the neighborhood of the Fermi level,

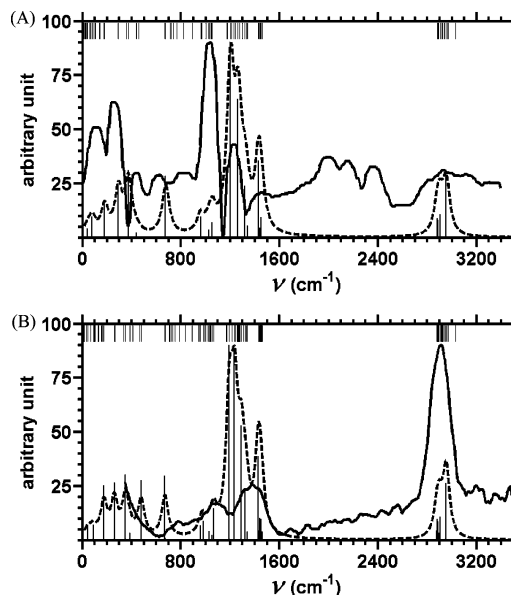


**Figure 1.** Comparison between calculated IETS (dashed curve) and experimental IETS (solid curve) for the **C8** molecule (A) and the **C11** molecule (B). The calculated IETS is simulated by broadening of the IETS peaks, however, ignoring the background ( $G_{el}^R + G_{el}^A$ ) in eq 15. The vertical lines under the dashed curve with the position representing the frequencies and the height of the intensities. Respectively, the broadening are 8.7 mV and 8.0 mV for the **C8** molecule and the **C11** molecule, which are ac modulation amplitude at which the experimental IETS are measured. The experimental IETS originate from Wang et al. (**C8**)<sup>6</sup> and Kushmerick et al. (**C11**).<sup>5</sup> Notice that the experimental IETS by Wang is defined as  $d^2I/dV^2$ , however, the one by Kushmerick is as  $(d^2I/dV^2)/(dI/dV)$ . The short vertical lines at top represent the vibrational frequencies of the molecules.

for the alkanedithiolates, are approximately 0.78 eV for the HOMO (highest occupied molecular orbital) and HOMO-1; 1.99 eV for HOMO-2 and HOMO-3; 2.07 eV for the LUMO (lowest occupied molecular orbital) and LUMO+1; and 2.67 eV for HOMO-4;<sup>47</sup> thus, only HOMO and HOMO-1 can be an effective conduction channel.

In this paper, we approximate the **C8** coupling between the conduction channel and a vibrational state by means of vibrational normal mode displacement between a neutral molecule and its corresponding positively charged state. However, this does not mean that we model the conduction state with a cation. The transport process is tunneling, which corresponds to no entity in our daily life, and no formal charging of the molecule takes place.

In Table 1, it lists the major normal mode displacements of the positively charged states of **C8** and **C11** from their neutral states.

We simulate IETS by the broadening of the IETS peaks of vibronic modes; however, we ignore the background ( $G_{el}^R + G_{el}^A$ ), which changes slowly with frequency. In Figure 1, it shows both the simulated IETS of **C8** and **C11** and their experimental IETS by Wang et al.<sup>6</sup> and by Kushmerick et al.,<sup>5</sup> respectively. Notice that both **C8** and **C11** are dithiolates in our calculation for the sake of symmetry of the junctions and similarity between **C8** and **C11**; however, the experimental IETS of **C11** is monothiolate and that of **C8** is dithiolate. We expect that this will not result in a significance difference. It could find that the simulated IETS shows similar structure for both the **C8** and **C11** molecules, with the region between 1000 and 1600 cm<sup>-1</sup> being the strongest IETS.

By comparison with the experimental IETS of the **C11** junction, both spectra depict a variety of well-resolved peaks

covering the vibrational energy, and the positions and shapes of the peaks are in good agreement with observed ones. The inconsistency is observed for the relative height of the peaks: the experimental peak around  $2900\text{ cm}^{-1}$  is much stronger than that of simulated one; peaks around  $1200\text{ cm}^{-1}$  are overestimated by our calculation. This discrepancy can be explained by the fact that the experimental background, the  $(G_{\text{el}}^{\text{R}} + G_{\text{el}}^{\text{A}})$  term in eq 15, is much larger at  $2900\text{ cm}^{-1}$  than at  $1200\text{ cm}^{-1}$ , and the full theoretical IETS peak intensity is the product of the  $(G_{\text{el}}^{\text{R}} + G_{\text{el}}^{\text{A}})$  term and the peak height contributed only by the vibronic coupling.

For the **C8** molecule, the simulated IETS shows similar structure to that of **C11**, however, the experimental IETS of **C8** seems in low quality compared to the **C11** because more disagreement exists between the simulated IETS and the experimental one. On the experimental IETS, three extra peaks between  $1800\text{ cm}^{-1}$  to  $2600\text{ cm}^{-1}$  and a few other peaks, which correspond to no vibrational modes, appear. These peaks are supposed to be caused by vibrational modes of the encasing  $\text{Si}_3\text{Ni}_4$  contamination by the original authors.<sup>6</sup> Although almost all peaks predicted by our calculation do appear on the experimental IETS, their relative heights differ. From these considerations and the good agreement of **C11** junction, it could be concluded that the quality of the experimental IETS of **C8** is quite low.

#### 4. Summary

We have present formalism for the IETS based on Green's function theory. The Green's function is calculated following the Dyson equation, and it is represented as a summation of the Green's function, where the electronic–vibronic coupling is not in action and where the electronic–vibronic coupling is in action. The integrated intensities of IETS peaks are correlated to electronic–vibronic coupling constant. A strong electronic–vibronic coupling between the neutral molecule and its positively charged states is supposed to be IETS active.

**Acknowledgment.** The author is indebted to Dr. Jeffrey R. Reimers who provided the program to calculate the electronic–vibronic coupling constant.

#### References and Notes

- Wolf, E. L. *Principles of electron tunneling spectroscopy*; Oxford University Press: New York, 1985; Vol. 71.
- Hipps, K. W.; Mazur, U. *J. Phys. Chem.* **1993**, *97* (30), 7803–7814.
- Lauhon, L. J.; Ho, W. *Rev. Sci. Instrum.* **2001**, *72* (1), 216–223.
- Stipe, B. C.; Rezaei, M. A.; Ho, W. *Science* **1998**, *280*, 1732–1735.
- Kushmerick, J. G.; Lazorcik, J.; Patterson, C. H.; Shashidhar, R. *Nano Lett.* **2004**, *4* (4), 639–642.
- Wang, W.; Lee, T.; Kretzschmar, I.; Reed, M. A. *Nano Lett.* **2004**, *4* (4), 643–646.
- Yu, L. H.; Keane, Z. K.; Ciszek, J.; Long, C.; Steward, M. P.; Tour, J. M.; Natelson, D. *Phys. Rev. Lett.* **2004**, *93* (26), 266802.
- Galperin, M.; Ratner, M. A.; Nitzan, A. *Nano Lett.* **2004**, *4* (9), 1605–1611.
- Ness, H.; Fisher, A. J. *Proc. Natl. Acad. Sci. U.S.A.* **2005**, *102* (25), 8826–8831.
- Persson, B. N. J.; Baratoff, A. *Phys. Rev. Lett.* **1987**, *59* (3), 339–342.
- Persson, B. N. J.; Demuth, J. E. *Solid State Commun.* **1986**, *57* (9), 769–772.
- Lorente, N.; Persson, M. *Phys. Rev. Lett.* **2000**, *85* (14), 2997–3000.
- Chen, Y.-C.; Zwolak, M.; DiVentra, M. *Nano Lett.* **2004**, *4* (9), 1709–1712.
- Ness, H.; Fisher, A. J. *Chem. Phys.* **2002**, *281* (2–3), 279–292.
- Troisi, A.; Ratner, M. A.; Nitzan, A. *J. Chem. Phys.* **2003**, *118* (13), 6072–6082.
- Galperin, M.; Ratner, M. A.; Nitzan, A. *Nano Lett.* **2005**, *5* (1), 125–130.
- Solomon, G. C.; Gagliardi, A.; Pecchia, A.; Frauenheim, T.; Carlo, A. D.; Reimers, J. R.; Hush, N. S. *J. Chem. Phys.* **2006**, *124* (9), 094704.
- Pecchia, A.; DiCarlo, A.; Gagliardi, A.; Sanna, S.; Frauenheim, T.; Gutierrez, R. *Nano Lett.* **2004**, *4* (11), 2109–2114.
- Troisi, A.; Ratner, M. A. *Nano Lett.* **2006**, *6* (8), 1784–1788.
- Landauer, R. *IBM J. Res. Dev.* **1957**, *1* (3), 223–231.
- Landauer, R. *Philos. Mag.* **1970**, *21*, 863–867.
- Buttiker, M.; Imry, Y.; Landauer, R.; Pinhas, S. *Phys. Rev. B* **1985**, *31* (10), 6207–6215.
- Datta, S. *Electronic Transport in Mesoscopic Systems*; Cambridge University Press: Cambridge, U.K., 1995.
- Yan, L.; Seminario, J. M. *Int. J. Quant. Chem.* **2007**, *107* (2), 440–450.
- Frisch, M. J.; Trucks, G. W.; Schlegel, H. B.; Scuseria, G. E.; Robb, M. A.; Cheeseman, J. R.; Montgomery, J. A., Jr.; Vreven, T.; Kudin, K. N.; Burant, J. C.; Millam, J. M.; Iyengar, S. S.; Tomasi, J.; Barone, V.; Mennucci, B.; Cossi, M.; Scalmani, G.; Rega, N.; Petersson, G. A.; Nakatsuji, H.; Hada, M.; Ehara, M.; Toyota, K.; Fukuda, R.; Hasegawa, J.; Ishida, M.; Nakajima, T.; Honda, Y.; Kitao, O.; Nakai, H.; Klene, M.; Li, X.; Knox, J. E.; Hratchian, H. P.; Cross, J. B.; Bakken, V.; Adamo, C.; Jaramillo, J.; Gomperts, R.; Stratmann, R. E.; Yazyev, O.; Austin, A. J.; Cammi, R.; Pomelli, C.; Ochterski, J. W.; Ayala, P. Y.; Morokuma, K.; Voth, G. A.; Salvador, P.; Dannenberg, J. J.; Zakrzewski, V. G.; Dapprich, S.; Daniels, A. D.; Strain, M. C.; Farkas, O.; Malick, D. K.; Rabuck, A. D.; Raghavachari, K.; Foresman, J. B.; Ortiz, J. V.; Cui, Q.; Baboul, A. G.; Clifford, S.; Cioslowski, J.; Stefanov, B. B.; Liu, G.; Liashenko, A.; Piskorz, P.; Komaromi, I.; Martin, R. L.; Fox, D. J.; Keith, T.; Al-Laham, M. A.; Peng, C. Y.; Nanayakkara, A.; Challacombe, M.; Gill, P. M. W.; Johnson, B.; Chen, W.; Wong, M. W.; Gonzalez, C.; Pople, J. A. *Gaussian 03*, revision C.02; Gaussian, Inc.: Pittsburgh, PA, 2004.
- Hohenberg, P.; Kohn, W. *Phys. Rev. B* **1964**, *136* (3), 864–871.
- Kohn, W.; Sham, L. J. *Phys. Rev.* **1965**, *140* (4A), A1133–A1138.
- Becke, A. D. *J. Chem. Phys.* **1993**, *98* (7), 5648–5652.
- Perdew, J. P.; Chevary, J. A.; Vosko, S. H.; Jackson, K. A.; Pederson, M. R.; Singh, D. J.; Fiolhais, C. *Phys. Rev. B* **1992**, *46* (11), 6671–6687.
- Perdew, J. P.; Wang, Y. *Phys. Rev. B* **1992**, *45* (23), 13244–13249.
- Wadt, W. R.; Hay, P. J. *J. Chem. Phys.* **1985**, *82* (1), 284–298.
- Hay, P. J.; Wadt, W. R. *J. Chem. Phys.* **1985**, *82* (1), 299–310.
- Hay, P. J.; Wadt, W. R. *J. Chem. Phys.* **1985**, *82* (1), 270–283.
- Hehre, W. J.; Stewart, R. F.; Pople, J. A. *J. Chem. Phys.* **1969**, *51* (6), 2657–2664.
- Wilson, E. B.; Decius, J. C.; Cross, P. C. *Molecular Vibrations*; McGraw-Hill: New York, 1955.
- Blom, C. E.; Atltona, C. *Mol. Phys.* **1976**, *31* (5), 1377–1391.
- Pulay, P.; Fogarasi, G.; Pang, F.; Boggs, J. E. *J. Am. Chem. Soc.* **1979**, *101* (10), 2550–1560.
- Pople, J. A.; Scott, A. P.; Wong, M. W.; Radom, L. *Isr. J. Chem.* **1993**, *33* (3), 345–350.
- Baker, J.; Jarzecki, A. A.; Pulay, P. *J. Phys. Chem. A* **1998**, *102* (8), 1412–1424.
- Rauhut, G.; Pulay, P. *J. Phys. Chem.* **1996**, *99* (10), 3093–3100.
- Pulay, P.; Fogarasi, G.; Pongor, G.; Boggs, J. E.; Vargha, A. *J. Am. Chem. Soc.* **1983**, *105* (24), 7037–7047.
- Halls, M. D.; Velkovski, J.; Schlegel, H. B. *Theor. Chem. Acc.* **2001**, *105* (6), 413–421.
- Hout, R. F.; Levi, B. A.; Hehre, W. J. *J. Comput. Chem.* **1982**, *3* (2), 234–250.
- Porter, M. D.; Bright, T. B.; Allara, D. L.; Chidsey, E. D. *J. Am. Chem. Soc.* **1987**, *109* (12), 3559–3568.
- Weber, P.; Reimers, J. R. *J. Phys. Chem. A* **1999**, *103* (48), 9830–9841.
- Reimers, J. R. *J. Chem. Phys.* **2001**, *115* (20), 9103.
- Seminario, J. M.; Yan, L. *Int. J. Quant. Chem.* **2004**, *102* (5), 711–723.
- Wang, W.; Lee, T.; Reed, M. A. *Phys. Rev. B* **2003**, *68*, 35416.